In $\sqrt{7} \times \sqrt{3}$ on Si(111): a nearly free electron metal in two dimensions

Eli Rotenberg[1], H. Koh[1], K. Rossnagel[1], H. W. Yeom[2], J. Schäfer[3], B. Krenzer[4], M. P. Rocha[4], S. D. Kevan[4]

[1] MS 6-2100, Advanced Light Source, Lawrence Berkeley National Laboratory, Berkeley, CA. 94720
[2] Institute of Physics and Applied Physics, Yonsei University,
134 Sinchon-dong, Seodaemun-gu, Seoul 120-749, Korea
[3] Institute of Physics, University of Augsburg, Universitätsstraße 1, D-86159 Augsburg, Germany
[4] Department of Physics, University of Oregon, Eugene, OR 97403
(Dated: August 8, 2003)

We present measurements of the Fermi surface and underlying bandstructure of a single layer of Indium on Si(111) with $\sqrt{7} \times \sqrt{3}$ periodicity. Electrons from both indium valence electrons and silicon dangling bonds contribute to a nearly free, two-dimensional metal on a pseudo-4-fold lattice, which is almost completely decoupled at the Fermi level from the underlying hexagonal silicon lattice. The mean free path inferred from our data is evidently limited only by the scattering at step edges, suggesting the system might be a suitable model for studying the ground state of two-dimensional metals.

Because of enhanced many-body interactions, quasi-two dimensional (2D) electron systems present diverse electronic phenomena such as charge density waves[1], metal-insulator transitions[2–4], Wigner lattices[5] and high-temperature superconductivity[6]. Metal monolayers on semiconductors might be attractive to study such phenomena, not only because their electronic states could be probed directly by surface-sensitive means, but also because their electrons could be confined to a single monolayer thickness. As such, they might approach an ideal two-dimensional limit, as opposed to quasi-2D systems such as layered compounds in which there remains significant interlayer coupling[7].

In this Letter, we report angle-resolved photoemission spectroscopy (ARPES) measurements of a model system, $\sqrt{7} \times \sqrt{3}$ Indium on Si(111), which displays a high degree of localization to the 2D layer and whose Fermi surface is strikingly close to the ideal 2D electron gas (2DEG). We show that the metallic layer's cohesion is so strong that nearly all the electrons available (Indium valence + Silicon dangling bonds) participate in the 2DEG with only a minority participating in covalent In-Si bonds. As a consequence of the confinement to the 2D layer, the potential felt by the electrons has nearly the pseudo-4-fold symmetry of the bare, isolated overlayer, with only minor effects arising from the hexagonal substrate symmetry. The mean free path for electron scattering at the Fermi level is quite long, suggesting that this system may be suitable for future investigations of the ground state properties of 2D metals.

A Si(111) crystal, miscut 2° towards $[11\bar{2}]$, was heated by direct current to obtain a 7×7 reconstruction. After depositing > 1.5 ML In and annealling to 500-600K to remove the excess In, we observed the $\sqrt{7} \times \sqrt{3}$ low energy electron diffraction (LEED) pattern shown in Fig. 1(a). Although 3 equivalent 120° rotated domains are possible, with careful annealling treatment, probably assisted by substrate step ordering, we reproducibly obtained the single-domain pattern shown in Fig. 1(a). The strongest recurring spots are those indicated by the large circles (inset), although the remaining $\sqrt{7} \times \sqrt{3}$ spots (small circles) can also be observed depending on the electron energy. Although Kraft et al[8, 9] reported the coexistence of 1.2 ML pseudo-4-fold (PFF) and 1.0 ML pseudo-6-fold phases, our x-ray photoelectron diffraction measurements[10] support a pure PFF phase. Apparently, our preparation method kinetically favors the 4-fold over the 6-fold phase.

After preparation, the samples were transferred *in vacuo* to a He-cooled goniometer capable of sample rotations along 2 orthogonal polar axes plus azimuth. Angle-resolved photoemission was performed with a hemispherical analyzer (Gammadata SES100) at beamline 7.0 of the Advanced Light Source. The total energy resolution (photons + electrons) was about 50 meV. The conversion from emission angle to 2-dimensional momentum is accomplished through a simple trigonometric transformation. The photon polarization was linear and lay in the scattering plane, roughly parallel to $[1\bar{1}0]$. The angular acceptance was about 0.15°. Samples were measured at 30-40K.

Fig. 1(b) shows the pseudo-4-fold (PFF) structure of the overlayer proposed by Kraft et al[8, 9]. It is notable that the rectangular overlayer symmetry differs so much from the hexagonal substrate. Although the overlayer is commensurate with the substrate over a large $\sqrt{7} \times \sqrt{3}$ unit cell, the overlayer-substrate arrangement appears locally incommensurate. Therefore it is useful to consider the corresponding reciprocal-space Brillocal Zone (BZ) as well as reciprocal lattice vectors $\mathbf{G}$ and basis vectors for three relevant symmetries found in this system (Fig. 1(c)): the fundamental $\sqrt{7} \times \sqrt{3}$ lattice, the bulk-terminated Si hexagonal lattice, and the reduced, rectangular PFF unit cell obtained if all In atoms were identical. These $\mathbf{G}$ vectors are denoted by (hk), (hk)H,
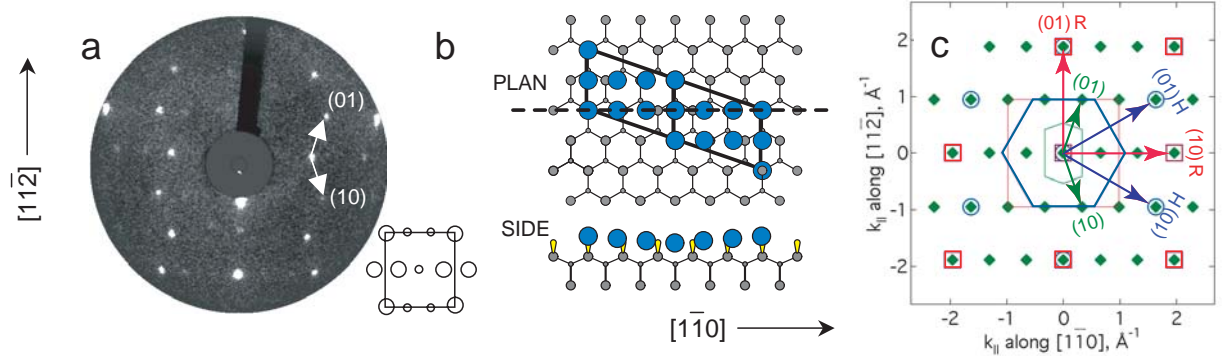
FIG. 1: Structural characterization of $\sqrt{7} \times \sqrt{3}$ Indium on Si(111). (a) LEED pattern at 144 eV. The inset indicates the strongest spots relative to the $\sqrt{7} \times \sqrt{3}$ Brillouin zone. (b) Plan view of the $\sqrt{7} \times \sqrt{3}$ unit cell of Indium atoms determined by Kraft *et al* [8, 9]. (c) The reciprocal lattice points **G**, the basis vectors ((hk)H, (hk)R, and (hk)) and Brillouin zones for unreconstructed 1×1, rectangular pseudo-4-fold, and $\sqrt{7} \times \sqrt{3}$ symmetries, respectively.

and (hk)R, respectively.

Fig. 2(a) shows a momentum map of the photoemission intensity from a narrow (≈ 150 meV) energy window centered on E_F. We find a striking array of nearly circular Fermi contours; the strongest of these represent a simple 2d metal on a nearly square lattice, which is discussed in many elementary solid state treatments. The raw data, taken over the quadrant $(k_x, k_y) > -0.5$ Å^{-1}, were mirror-symmetrized across these axes (although not strictly a mirror plane, we observed approximate mirror symmetry across the k_x axis).

To model the observed Fermi surface, we used a simple plane wave pseudopotential model in which the potential is projected onto reciprocal space as $V(\mathbf{r}) = \sum_\mathbf{G} V_\mathbf{G} e^{i\mathbf{G}\cdot\mathbf{r}}$ such that nearly free electron bands with dispersion

$$E = (\hbar^2/2)(k_x^2/m_x^* + k_y^2/m_y^*) \qquad (1)$$

are found centered on each possible **G** vector of the reciprocal lattice. Thirty-nine **G** vectors (some equivalent by symmetry) were sufficient to account for practically all the features in the experimental intensity map. This calculation together with the data are shown in Fig. 2(b), in which the experimental data has been appropriately symmetrized (translation + reflection) into the reduced $\sqrt{7} \times \sqrt{3}$ Brillouin zone.

Choosing the effective masses $m_{x,y}^* = (1.1e, 1.08e)$ and the Fermi energy (6.9 eV) brings the data and model into excellent agreement along the broad circular arcs. Only one principle pseudopotential coefficient (discussed further below), is needed to account for the anticrossing gap labelled 'a' in Fig. 2(b). Conversely, the model and data differ significantly at the central "butterfly" feature in two ways. The first is that the experimental butterfly "wings" are much larger than that of the model, leading the predicted position of gap a to differ from the experiment. A second, more important difference is the presence of two elliptical protrusions S_1 not predicted by the simple model, which we will return to later.

We now consider the nature of the In-Si chemical bond and its influence on the Fermi surface topology. In the PFF unit cell there is one In atom (of valence 3) and 5/6 unsaturated Si atoms (contributing 1 electron each) for a total of 3.833 electrons. We find the central circular contour ('c' in Fig. 2(a)) to cover 1.725 times the PFF BZ, or 3.45 electrons per Indium atom, far in excess of the 3 available Indium valence electrons. Although some additional charge might come from bulk electrons trapped at the surface by a band-bending potential [11], the charge density associated with such accumulation layers is far too small (typically 10^{11} e/cm^2) to account for the excess charge.

We conclude that the 2D metal has contributions not only from the In atoms but also from about half of the surface silicon dangling bonds. This is not unreasonable considering the structural model in Fig. 1(b). The diverse In-Si arrangements suggest the possibility of multiple types of In-Si bonds. Each interfacial Si atom contributes a single protruding dangling bond electron, some of which bond covalently with overlying indium atoms, and some of which may protrude into their interstices. We speculate that these interstitial dangling bonds are donated to the charged layer, increasing the electron count from 3 to 3.45 electrons per Indium atom. This is a very surprising kind of bond, much more characteristic of metallic bonding than the directional covalent bonding expected of semiconductors. The large gain in cohesive energy by this charge donation to the In layer must offset the large energy loss associated with vacating the dangling bond. These findings confirm that the dominant interaction determining the structure is metallic In-In and not covalent In-Si bonding[8, 9]. Since Indium does not form a bulk silicide then this is an example of a purely 2D metallic silicide.

The remaining dangling bonds participate in a more conventional In-Si covalent bond. This appears to be the origin of the extra S_1 features in Fig. 2(b), which
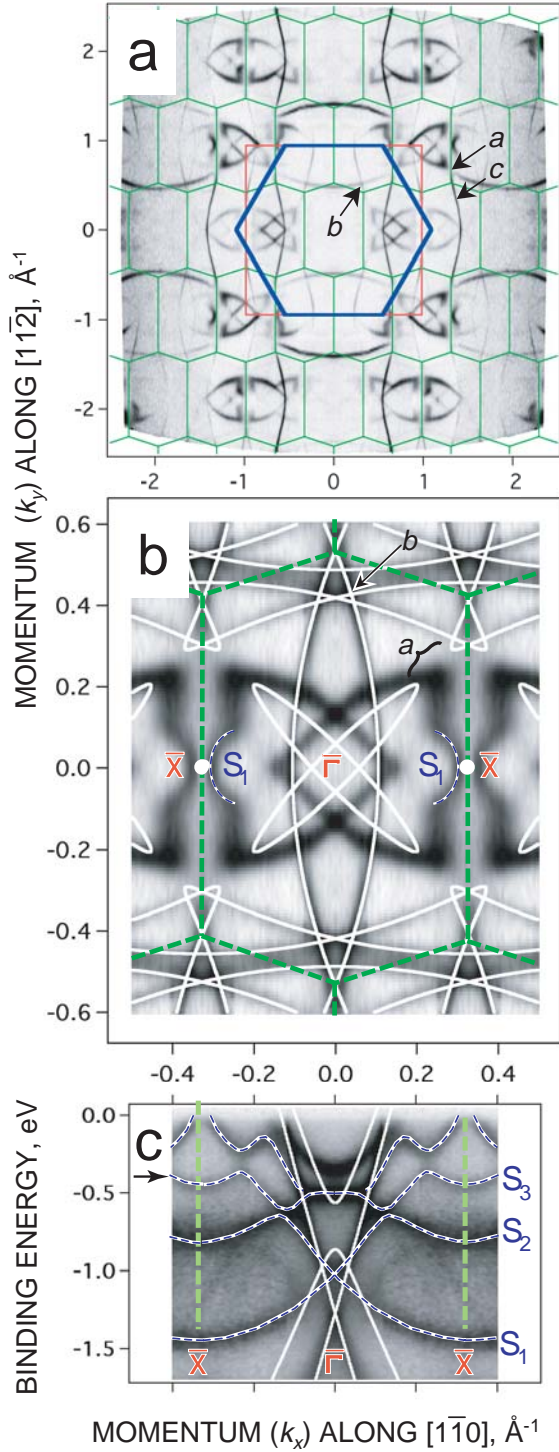
FIG. 2: Fermi contours and underlying bands of $\sqrt{7} \times \sqrt{3}$ Indium on Si(111). (a) The intensity at E_F for $h\nu$=89.5 eV, together with Brillouin zones from Fig. 1. Raw data are shown in the upper right quadrant. The rest of the data are obtained by mirror symmetry operations. (b) The experimental data of (a) averaged over each $\sqrt{7} \times \sqrt{3}$ Brillouin zone according to tranlational/reflection symmetry, together with a plane-wave calculation for $\sqrt{7} \times \sqrt{3}$ symmetry as described in the text. (c) The measured electronic bands similarly backfolded in the reduced BZ for the line $k_y = 0$. The overplotted bands are: solid=simulated; dashed=guides to the eye. The top of the bulk Silicon valence band maximum is indicated by an arrow.

cannot be accounted for by our simple nearly free electron model (white lines). In contrast to these minor alterations to the Fermi contours, the underlying bandstructure (Fig. 2(c)) is quite surprising: a set of three parabolic bands (S_{1-3}) are observed; not only mixing with each other, these states apparently mix with the free-electron bands near $\overline{\Gamma}$, effectively raising the effective mass of these states there. This therefore accounts for the enlargement of the "butterfly" wings centered on $\overline{\Gamma}$ compared to our model.

How many electrons are represented by S_{1-3}? Considering the wide range of these states along [$1\overline{1}0$] (see Fig. 2(c)) and along [$11\overline{2}$] (about 20% of the $\sqrt{7} \times \sqrt{3}$ BZ), we can conservatively estimate at least 0.3 electrons per Indium atom. Together with the 0.45 electrons donated directly to the free-electron bands, we have more or less accounted for the 5/6 =0.833 electrons expected from Si dangling bonds.

If the electrons are mostly confined to the In layer, then they should "feel" the PFF symmetry more than the hexagonal symmetry of the substrate. In our model we find a circular Fermi contour centered on each $V_\mathbf{G}$. Since the observed photoemission intensity for a circle centered at $\mathbf{G}$ goes as the square of the corresponding $V_\mathbf{G}$ [12], then by inspection of Fig. 2(a), we can rank the potential at $\mathbf{G}$=(11)R as the most important followed by $\mathbf{G}$=(01)R, (10)R, (01)H, and then all the others. Although additional circles are found centered on practically all the other, higher symmetry $\sqrt{7} \times \sqrt{3}$ $\mathbf{G}$s, they are much weaker and observable only in unconnected sections of arc. This shows that the pseudopotentials associated with the rectangular In lattice greatly dominate the potential (the ratio of intensity between strongest and weakest features is on the order of 10-20).

Quantitative estimates of $V_\mathbf{G}$ in this fashion are difficult since the photoemission intensities are subject to strong systematic energy-dependent intensity deviations (similar to those in the LEED patterns[13, 14]). Absolute measurements of $V_\mathbf{G}$ are possible because of the mixing of bands whose centers are connected by $\mathbf{G}$. This mixing results in anticrossing gaps in energy and momentum (e.g. gap a in Fig. 2(a,b)). In order to reproduce this gap we used a value $V_{(11)R}$=0.15 eV for our simulation. Apart from this anticrossing gap a, there is no experimentally resolved gap at E_F for any other potential terms $V_\mathbf{G}$, which must all therefore be less than about 25 meV.

At deeper binding energies, on the other hand, we found gaps at several other crossings; for example, the potential term $V_{(01)H}$ (affecting the b intersection in Fig. 2(a)) was found to induce a gap for binding energies greater than 0.8 eV. This makes sense because as the bands come into resonance with the underlying bulk Si bands, their wavefunctions penetrate deeper towards the substrate and therefore the potential terms associated with the hexagonal silicon lattice become more important.

Some authors [14, 15] have described the presence of such weak replica bands as we see in Fig. 2 as due not to weak potentials $V_{\mathbf{G}}$ felt by the electron in the initial state, but rather as a consequence of final state surface Umklapp scattering from the corresponding surface $\mathbf{G}$ vectors. Normally, surface Umklapp scattering is ascribed as the third step in a three step model for photoemission from bulk bands (excitation, transport to the surface, scattering by the surface potential). We conservatively assign the replica bands to initial-state potential effects; however, in the absence of anticrossing gaps for the weak replica bands, it remains difficult to eliminate final state scattering as their cause. To the extent this occurs, it strengthens our claim that the potential contribution of the substrate symmetry is negligible.

The images in Figs. 2(a,b) are comprised of the sharpest Fermi contours in our experience, which attests to the high quality of the films and long mean free paths of the carriers. These properties ultimately derive from the large energy difference between the Fermi level and the silicon states. Our measurements indicate that the Fermi level of the 2D metal is pinned about 0.4 eV above the silicon valence band maximum (arrow in Fig. 2(c)). Since this is near midgap, this surface represents about the best localization of electrons to the surface layer which can be achieved on silicon. The momentum width δk perpendicular to the Fermi contour (point c of Fig. 2(a)) is about 0.01 Å^{-1} which is nearly limited by our angular resolution. We therefore conclude the mean free path for electron scattering is in excess of $1/\delta k = 100$ Å[16]. Since the average step-step distance along the electron path that we measured was only ~ 430 Å, this suggests that the carrier lifetimes are mainly determined by scattering at step edges, and that the lifetime is much longer within the terraces.

Currently the zero-field ground state of two dimensional electron gases is controversial, as is the relative roles of disorder, pairing interactions, and electron-electron correlation[4]. Considering the high electron density (3.6×10^{15} cm^{-2}), electron-electron interactions should be screened out and in the inevitable presence of defects the ground state should be insulating[17, 18]. On the other hand pairing is still important: our temperature dependent valence band linewidths[19] (not shown) indicate an electron-phonon coupling constant $\lambda \simeq 1$, similar to that of bulk Indium. We might therefore expect the surface to become superconducting near the critical temperature of bulk In ($T_{\mathrm{c}} = 3.4$ K). We propose that temperature-dependent measurements as a function of defect density (controlled by adsorbate depostion) may clarify the zero-field two-dimensional ground state.

In summary, extensive high-resolution bandstructure measurements, supported by simulations, show that the electronic structure of $\sqrt{7}\times\sqrt{3}$ In/Si(111) consists of two manifolds of bands. Most electrons are found in a nearly-free-electron metallic band on a pseudo-4-fold (PFF) lattice potential, with a minority of electrons in a second set of bands ascribed to covalent In-Si bonds. Coupling between the dominant free-electron gas and the remaining interface states is confined to a relatively small part of the Fermi surface near $\overline{\Gamma}$ where the bulk valence band edge comes closest to the Fermi level. The mean free path inferred from our data is evidently limited only by the scattering at step edges, reflecting the very high quality of films grown. These films may be suitable for studying ground state properties of low dimensional metals.

[1] G. Grüner, *Density Waves in Solids* (Addison-Wesley, Massachusetts, 1994).
[2] P. W. Anderson, Phys. Rev. **109**, 1492 (1958).
[3] S. V. Kravchenko, G. V. Kravchenko, J. E. Furneaux, V. M. Pudalov, and M. D'Iorio, Phys. Rev. B **50**, 8039 (1994).
[4] M. S. E. Abrahams, S. Kravchenko, Reviews of Modern Physics **73**, 251 (2001).
[5] E. P. Wigner, Phys. Rev. B **46**, 1002 (1934).
[6] G. Bednorz and K. A. Müller, Z. Phys. B **64**, 189 (1986).
[7] K. Rossnagel, L. Kipp, M. Skibowski, C. Solterbeck, T. Strasser, W. Schattke, D. Voß, P. Krüger, A. Mazur, and J. Pollmann, Phys. Rev. B **63**, 125104 (2001).
[8] J. Kraft, S. L. Surnev, and F. P. Netzer, Surf. Sci. **340**, 36 (1995).
[9] J. Kraft, M. G. Ramsey, and F. P. Netzer, Surf. Sci. Lett. **372**, L271 (1997).
[10] E. Rotenberg, H. W. Yeom, S. Takeda, et al., Symp. Mater. Res. Soc. 2001 P **648**, 10 (2001).
[11] D. C. Tsui, Phys. Rev. Lett. **24**, 303 (1970).
[12] E. Rotenberg, W. Theis, and K. Horn, Journal of Alloys and Compounds **342**, 348 (2002).
[13] R. Losio, K. N. Altmann, and F. J. Himpsel, Phys. Rev. B **61**, 10845 (2000).
[14] H. J. Neff, I. Matsuda, M. Hengsberger, F. Baumberger, T. Greber, and J. Osterwalder, Phys. Rev. B **64**, 235415 (2001).
[15] J. N. Crain, K. N. Altmann, C. Bromberger, and F. J. Himpsel, Phys. Rev. B **66**, 205302 (2002).
[16] D. Y. Petrovykh, K. N. Altmann, H. Höchst, M. Laubscher, S. Maat, and G. J. Mankey, Appl. Phys. Lett. **73**, 3459 (1998).
[17] E. Abrahams, P. W. Anderson, D. C. Licciardello, and T. V. Ramakrishnan, Phys. Rev. Lett. **42**, 673 (1979).
[18] A. R. Hamilton, M. Y. Simmons, M. Pepper, E. H. Linfield, P. D. Rose, and D. A. Ritchie, Phys. Rev. Lett. **82**, 1542 (1999).
[19] T. Balasubramanian, E. Jensen, X. L. Wu, and S. L. Hulbert, Phys. Rev. B **57**, 6866 (1998).